

3 **An Analysis of Axial Couette Flow in**
4 **Annular Region of Abruptly Stopped**
5 **Pipes**

6
7 **ABSTRACT**
8

Aims: Flow in annular regions encounters in many fields such as bio-medical, petroleum, aerospace and chemical industries and among them, the flow between two coaxial pipes has rather become interesting due to its asymmetry nature.

Study design: Theoretical solution and numerical approximation and analysis.

Place and Duration of Study: Department of mathematics, Faculty of Science, University of Peradeniya, Sri Lanka, between August 2017 and January 2018.

Methodology: Yet it is particularly challenging to obtain theoretical solutions. In this paper, we carried out a comprehensive analysis for unsteady, unidirectional and incompressible Couette flow between annulus, when inner and outer pipes were brought to abrupt stop from constant velocities. The velocity of the field is derived by applying the Laplace transformation method. The analytical work is supported by the numerical approximation using Finite Difference Method for the same fluid, which was implemented in MATLAB programming. We illustrate results varying radii of the outer and inner pipe captured by ratio ($\eta = 0.1, 0.3, 0.5$ and 0.7) and for different boundary conditions. Flow field was visualized using FDM approximation for selected parameter regime when the flow was suddenly stopped.

Results: Asymmetry of the velocity profile was affected by different radius ratios ($\eta = 0.1, 0.3, 0.5$ and 0.7). Unsteadiness in the flow field was happened due to sudden changes in flow parameters.

Conclusion: The results depicted that radii ratio and boundary condition has a strong impact on the role on changing the flow characteristics and flow parameters.

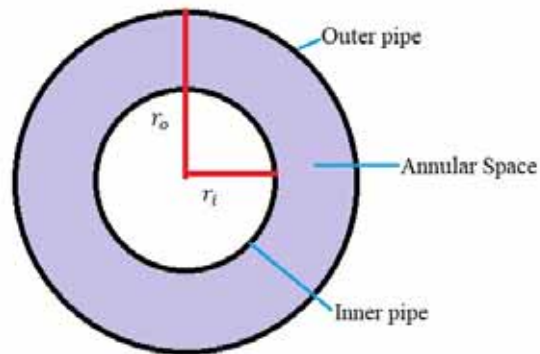
9
10 *Keywords: Couette flow, Asymmetry velocity, Navier-Stokes equations, Radii ratios*
11
12

13 **1. INTRODUCTION**
14

15 The study of flow through an annulus bounded by two coaxial pipes has attracted the attention of
16 researches due to its peculiarity nature and the flow geometry is one which has found considerable
17 practical application in the process industries. The concentric annulus also presents a flow system
18 which is still amenable to analysis. Nevertheless, in this seemingly simple flow field some rather
19 strange and puzzling phenomena occur. The most interesting of these are associated with the
20 transition from laminar to non-laminar [1].

21 The unsteady laminar Couette flow in concentric annulus, where the geometry is shown in , is
22 investigated to predict the surge or swab pressure encountered when running or pulling pipes in a
23 liquid-filled borehole. The motion equations were analytically solved in [2] for power-law fluids by the
24 perturbation method. During the drilling operation of oil and gas wells, the velocity field varies along
25 the well length and the resulting flow model is three-dimensional. Lubrication theory has been used to
26 simplify the governing equations into a two dimensional differential equation that describes the
27 pressure field and velocity in each cross section was analysed for different cases in [3]. In [4], stability
28 and transition to turbulence of wall-bounded unsteady velocity profiles with reverse flow was
29 investigated. Experiment and theoretical investigations of instability and evolution of reverse flow that
30 occurred in a decelerating flow has been performed where the flow is generated by the controlled
31 piston motion. The procedure to obtain analytical solution for unsteady laminar flow in an infinitely

32 long pipe with circular cross section and in an infinitely long two dimensional channel, created by an
33 arbitrary but given volume flow rate with time was presented in [5].



34 **Fig. 1. Schematic description of annular space bounded by concentric pipes (radius of the**
35 **inner pipe: r_i and radius of the outer pipe: r_o)**
36

37 Some properties of the time dependent Navier-Stokes equation for impulsively started from rest by
38 sudden application of a constant pressure gradient or by the impulsive motion of a boundary was
39 discussed in [6] and a satellite reaction control subsystem was explained in [7]. A flow channel
40 network numerical scheme is used to determine the blow down pressure profile and the steady state
41 pressure drops in the propellant lines. This study give the idea about damaged to the propulsion
42 components or lines due to the sudden closure of fuel valves.

43 Finite difference method was applied for fully developed flat plate flow, circular pipe flow and square
44 duct flow [8]. Pressure drop characteristics of turbulent flow through 90 degree pipe bends were
45 numerically investigated and pressure distribution for various Reynolds number and curvature ratio
46 was analyzed [9].

47 Moreover, an analytical solution to the flow through the pipe and the annular space between two
48 concentric pipes has been obtained for the case of one-dimensional unsteady flow in [10]. However,
49 the solution obtained were only when the volume flow rate is provided. Analytical solution of the
50 unsteady laminar bi-directional flow between concentric pipes with known volume flow rate has been
51 derived for various cases in [11]. A new analytical solution for unsteady bi-directional flow through an
52 annulus between two concentric pipes with a prescribed time dependent volume flow rate has also
53 been obtained in [12]. Analytically obtained velocity profiles are compared with experimental data and
54 also numerical results [11] and they are used for determining the linear stability characteristics of such
55 flows. Yet, the analysis when annular boundaries have abrupt changes is still scarce.

56 In the present work, we carry out an analysis of suddenly stopped Couette flow. Initially the flow was
57 considered as independent of time and subsequently, the pipes were brought to abrupt rest and the
58 flow then depends on time. This sudden change in boundaries encounters in many industrial
59 processes. Asymmetry, radii ratio and unsteadiness of the annular flow have significant but different
60 role in flow instability and transition.

61 The paper is organized as follows. In section 2, the unsteady and incompressible flow in a concentric
62 annulus for abruptly stopped axial Couette flow is investigated. Exact analytical solution methodology
63 for incompressible, unidirectional and unsteady flow is presented. In section 3, Finite Difference
64 Method is discussed to approximate the flow characteristics in the annular region and the
65 approximate values for axial Couette flow for various cases are presented. In section 5, the present
66 work and the scope for future work were summarized.

67 68 **2. METHODOLOGY**

69 70 **2.1 Theoretical Implementation**

71
72 An annular region between a long inner pipe of radius, r_i^* and a coaxial outer pipe of radius, r_o^* is
73 considered in the study. The flow is taken to be at steady state in the annular region, before making
74 the abrupt changes to the boundary. Cylindrical co-ordinates system (r^*, θ, x^*) is employed due and,
75 r^* , θ , and x^* indicates the radial, azimuthal and axial directional co-ordinates respectively.
76 Corresponding velocity components in axial, radial and azimuthal directions are defined as v_r^* , v_θ^* and

77 v_x^* respectively. The superscript “*” is used to denote dimensional quantities. The simplified Navier-
 78 Stokes equation was written as when the flow was assumed to be axisymmetric, incompressible,
 79 unidirectional, fully developed, entirely depend on the wall movement (no-slip boundary condition) and
 80 has no body force. Hence, simplified Navier-Stokes equations for steady and unsteady flow are as
 81 below in equations (1) and (2) respectively.

$$\frac{1}{r^*} \frac{\partial}{\partial r^*} \left(r^* \frac{\partial v_x^*}{\partial r^*} \right) = 0 \quad (1)$$

$$\rho \left(\frac{\partial v_x^*}{\partial t^*} \right) = \mu \left[\frac{1}{r^*} \frac{\partial}{\partial r^*} \left(r^* \frac{\partial v_x^*}{\partial r^*} \right) \right] \quad (2)$$

82 Dimensionless parameters introduced with special co-ordinates are normalized by Re (Reynolds
 83 number), while velocity and time are made dimensionless by U_c and $\frac{U_c}{R_c}$, respectively; where, R_c and U_c
 84 were characteristic length and velocity respectively. Thus, the non-dimensional variables and
 85 parameters are written as,

$$v_x = \frac{v_x^*}{U_c}; \quad r = \frac{r^*}{R_c}; \quad t = \frac{t^* U_c}{R_c}; \quad Re = \frac{U_c R_c \rho}{\mu} \quad (3)$$

86
 87
 88

2.1.1 Steady State Solution

$$v_x(r, 0) = C_1 + C_2 \ln(r) \quad (4)$$

$$v_x(r_i, t) = V_i; \quad v_x(r_o, t) = V_o \quad (5)$$

89 Equations (4) and (5) were dimensionless initial and inner and outer boundary conditions respectively
 90 for steady governing equation. Where, initial condition was obtained from the literature study in [13]
 91 and boundary conditions were assumed as constant velocities.

92 Hence, the solution for the steady state equation can be written as,

$$v_x(r, t) = \frac{V_o - V_i}{2} + \frac{V_i - V_o}{2 \ln(\eta)} [2 \ln(r) - \ln(r_o r_i)] \quad (6)$$

93 Let,

$$D_1 = \frac{V_o + V_i}{2}; \quad D_2 = \frac{V_i - V_o}{2 \ln(\eta)} \ln(r_o r_i); \quad D_3 = \frac{V_i - V_o}{\ln(\eta)} \quad (7)$$

94 And, $D_{12} = D_1 - D_2$. Thus, the simplified steady state solution is written as,

$$v_x = D_{12} + D_3 \ln(r) \quad (8)$$

95
 96
 97

2.1.2 Unsteady Solution

$$v_x(r, 0) = D_{12} + D_3 \ln(r) \quad (9)$$

$$v_x(r_i, t) = F_i; \quad v_x(r_o, t) = F_o \quad (10)$$

98 The equations (9) and (10) are dimensionless initial and inner and outer boundary conditions
 99 respectively for unsteady governing equation. Initial condition for the unsteady equation is the solution
 100 of the steady state equation.

101 Laplace transforms of dimensionless unsteady equation and boundary conditions are,

$$\frac{d^2 \bar{v}_x(r, s)}{dr^2} + \frac{1}{r} \frac{d \bar{v}_x(r, s)}{dr} - Re s \bar{v}_x(r, s) = -Re v_x(r, 0) \quad (11)$$

$$\bar{v}_x(r_i, s) = \bar{F}_i; \quad \bar{v}_x(r_o, s) = \bar{F}_o \quad (12)$$

102 Here, the over bar quantities were transformed variables. Hence, $v_x(r, 0) = D_{12} + D_3 \ln(r)$ is due to
 103 the choice of initial condition. The equation (11) is a second order, non-homogeneous and ordinary
 104 differential equation. Since the governing equation and boundary conditions are known, the problem
 105 was well posed.

$$\frac{d^2 \bar{v}_x(r, s)}{dr^2} + \frac{1}{r} \frac{d \bar{v}_x(r, s)}{dr} - Re s \bar{v}_x(r, s) = -Re [D_{12} + D_3 \ln(r)] \quad (13)$$

106 Here, $Re s = q^2$. In the equation (13), the homogeneous part is the modified Bessel equation of
 107 highest order [13,14]. Homogeneous and non-homogeneous solutions are,

$$\bar{v}_{x \text{ homogeneous}} = \phi_1 I_0(qr) + \phi_2 K_0(qr) \quad (14)$$

$$\bar{v}_{x \text{ non-homogeneous}} = -[D_{12} + D_3 \ln(r)] \quad (15)$$

108 Thus, the complete solution is,

$$\bar{v}_x = \phi_1 I_0(qr) + \phi_2 K_0(qr) - [D_{12} + D_3 \ln(r)] \quad (16)$$

109 Here, I_0 and K_0 are highest order modified Bessel functions of first and second kind respectively. ϕ_1
 110 and ϕ_2 were the arbitrary constants, determined by using boundary conditions (10) in equation (16).

111 To find the non-homogeneous solution, Wronskian [15] is given as,

112

$$W[I_0(qr), K_0(qr)] = \begin{vmatrix} I_0(qr) & K_0(qr) \\ I_0'(qr) & K_0'(qr) \end{vmatrix} = -\frac{1}{r} \quad (17)$$

$$\bar{v}_{x1non-homogeneous} \quad (18)$$

$$= -I_0(qr) \int \frac{\left\{ \begin{matrix} K_0(qr) \\ [-Re D_3 \ln(r)] \end{matrix} \right\}}{-\frac{1}{r}} dr$$

$$+ K_0(qr) \int \frac{\left\{ \begin{matrix} I_0(qr) \\ [-Re D_3 \ln(r)] \end{matrix} \right\}}{-\frac{1}{r}} dr$$

$$\bar{v}_{x2non-homogeneous} = -I_0(qr) \int \frac{\left\{ \begin{matrix} K_0(qr) \\ [-Re D_{12}] \end{matrix} \right\}}{-\frac{1}{r}} dr + K_0(qr) \int \frac{\left\{ \begin{matrix} I_0(qr) \\ [-Re D_{12}] \end{matrix} \right\}}{-\frac{1}{r}} dr \quad (19)$$

113 Thus, the non-homogeneous solution is written as,

$$\bar{v}_{xnon-homogeneous} = \bar{v}_{x1non-homogeneous} + \bar{v}_{x2non-homogeneous} \quad (20)$$

114 From equation (16), the solution in transformed domain is written as,

$$\bar{v}_x = \phi_1 I_0(qr) + \phi_2 K_0(qr) + \frac{D_{12}}{s} + \frac{D_3 \ln(r)}{s} \quad (21)$$

115 Applying the boundary conditions (12) in the equation (21), we can find the arbitrary constants ϕ_1 and
116 ϕ_2 . Then the equation (21) was written as,

$$\bar{v}_x = \left\{ \frac{\left(\begin{matrix} \left[\bar{F}_i - \frac{D_{12}}{s} - \frac{D_3 \ln(r_i)}{s} \right] [I_0(qr_o)K_0(qr) - K_0(qr_o)I_0(qr)] \\ + \left[\bar{F}_o - \frac{D_{12}}{s} - \frac{D_3 \ln(r_o)}{s} \right] [K_0(qr_i)I_0(qr) - I_0(qr_i)K_0(qr)] \end{matrix} \right)}{K_0(qr_i)I_0(qr_o) - I_0(qr_i)K_0(qr_o)} \right\} \quad (22)$$

$$+ \left[\frac{D_{12} + D_3 \ln(r)}{s} \right]$$

117 If the boundary conditions are constants, then $\bar{F}_i = \frac{F_i}{s}$ and $\bar{F}_o = \frac{F_o}{s}$.

$$qr_i = r_i \sqrt{Re} \sqrt{s} = A\sqrt{s}; \quad qr_o = r_o \sqrt{Re} \sqrt{s} = B\sqrt{s}; \quad qr = r \sqrt{Re} \sqrt{s} = C\sqrt{s} \quad (23)$$

118 Here, $= r_i \sqrt{Re}$; $B = r_o \sqrt{Re}$ and $C = r \sqrt{Re}$.

119 The flow velocity is,

$$\bar{v}_x = \left\{ \frac{\left(\begin{matrix} \left[\bar{F}_i - \frac{D_{12}}{s} - \frac{D_3 \ln(r_i)}{s} \right] \\ [I_0(B\sqrt{s})K_0(C\sqrt{s}) - K_0(B\sqrt{s})I_0(C\sqrt{s})] \\ + \left[\bar{F}_o - \frac{D_{12}}{s} - \frac{D_3 \ln(r_o)}{s} \right] \\ [K_0(A\sqrt{s})I_0(C\sqrt{s}) - I_0(A\sqrt{s})K_0(C\sqrt{s})] \end{matrix} \right)}{s [K_0(A\sqrt{s})I_0(B\sqrt{s}) - I_0(A\sqrt{s})K_0(B\sqrt{s})]} \right\} + \left[\frac{D_{12} + D_3 \ln(r)}{s} \right] \quad (24)$$

120

121 Moreover, the solution in time domain $v_x(r, t)$ was obtain by taking the inverse Laplace transform
122 of $\bar{v}_x(r, s)$. The inverse transform of equation (24) can be obtained using the convolution theorem.

123 Applying convolution theorem to equation (24), we can obtain,

$$v_x(r, t) = \frac{1}{2\pi i} \int_{r-i\infty}^{r+i\infty} \bar{v}_x(r, s) \exp(r, s) dt \quad (25)$$

124 We can write the integrand in the form of $\frac{a\Gamma^{n+1}}{b\Gamma^n}$, where, Γ is the radius of the Bromwich contour taken;

125 such that all the poles lie in the left of the contour. The integrand diverges as $\Gamma \rightarrow \infty$, preventing the

126 application of the convolution theorem, Hence, we take the inverse Laplace transform [16] of equation
 127 (24) and obtain the solution in time domain.

$$v_x(r, t) = \sum \left\{ \text{residue of poles of } [\bar{v}_x(r, s) \exp(r, s)] \right\} \quad (26)$$

128 Thus, the complete final solution was written as,

$$v_{x_1} = \left\{ \frac{\pi r_o^2 Re [F_i - D_{12} - D_3 \ln(r_i)] \begin{bmatrix} Y_0(a_n) J_0\left(\frac{C}{B} a_n\right) \\ -J_0(a_n) Y_0\left(\frac{C}{B} a_n\right) \end{bmatrix} \exp\left(-\frac{a_n^2 t}{r_o^2 Re}\right)}{2a_n^2 \left(\frac{dD}{dS}\right)_{s=-\frac{a_n^2}{B^2}}} \right\} \quad (27)$$

$$+ \frac{\ln \frac{r}{r_o}}{\ln \frac{A}{B}} \left[\bar{F}_i - \frac{D_{12}}{s} - \frac{D_3}{s} \ln(r_i) \right]$$

$$v_{x_2} = \left\{ \frac{\pi r_o^2 Re [F_o - D_{12} - D_3 \ln(r_o)] \begin{bmatrix} J_0\left(\frac{A}{B} a_n\right) Y_0\left(\frac{C}{B} a_n\right) \\ -Y_0\left(\frac{A}{B} a_n\right) J_0\left(\frac{C}{B} a_n\right) \end{bmatrix} \exp\left(-\frac{a_n^2 t}{r_o^2 Re}\right)}{2a_n^2 \left(\frac{dD}{dS}\right)_{s=-\frac{a_n^2}{B^2}}} \right\} \quad (28)$$

129 and

$$v_{x_3} = D_{12} + D_3 \ln(r) \quad (29)$$

130 Thus, the velocity in time domain:

$$v_x(r, t) = v_{x_1} + v_{x_2} + v_{x_3} \quad (30)$$

131 When F_i and F_o are assumed to be zero in the equation (30), the exact analytical solution is obtained
 132 for the abruptly stopped axial Couette flow. Note that, since the flow was entirely depend on the wall
 133 movement, the pressure difference throughout the annulus in axial direction was not considered. A
 134 numerical implementation was carried out to visualize the flow field for different ratios.

135

136 2.2 Numerical Implementation

137

138 The numerical implementation, starts with the non-dimensional form of equation (2), where the
 139 dependent variable, v_x (velocity in axial direction) and the independent variables, r (radius between
 140 inner and outer pipes) and t (time). To approximate the solution of the unsteady equation using Finite
 141 Difference method, solution of the steady state equation was taken as initial condition (9).

142 Using central space difference approximation the second order partial derivative with respect to radius
 143 and the first order partial derivative with respect to radius of the equations are approximated as,

$$v_x''(r) \approx \left\{ \frac{\left[\frac{U(r - \Delta r) - 2U(r)}{\Delta r} + \frac{U(r + \Delta r) - U(r)}{\Delta r} \right]}{(\Delta r)^2} \right\} + O(\Delta r)^2 \quad (31)$$

$$v_x'(r) \approx \left[\frac{U(r + \Delta r) - U(r - \Delta r)}{2\Delta r} \right] + O(\Delta r)^2 \quad (32)$$

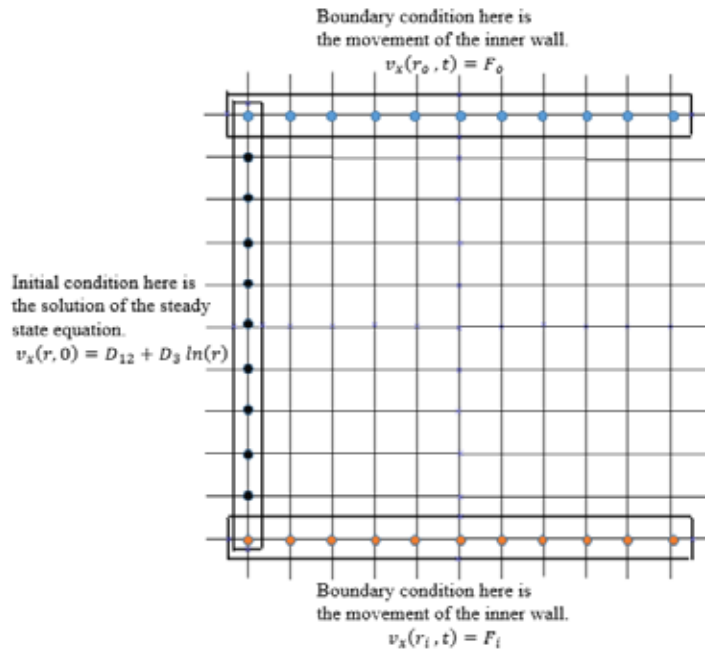
144 Using the forward time difference approximation the first order partial derivative with respect to time is
 145 approximated as,

$$v_x'(t) \approx \left[\frac{U(t + \Delta t) - U(t)}{\Delta t} \right] + O(\Delta t)^2 \quad (33)$$

146 Thus, the discretized equation with $\Delta t = k$ and $\Delta r = h$ is as,

$$\frac{v_{x_{i,j+1}} - v_{x_{i,j}}}{k} = \frac{1}{Re} \left\{ \frac{\left[\frac{\left(v_{x_{i+1,j}} - 2v_{x_{i,j}} \right) + v_{x_{i-1,j}}}{h^2} \right]}{\left[\frac{1}{r} \left[\frac{v_{x_{i+1,j}} - v_{x_{i-1,j}}}{2h} \right] \right]} \right\} \quad (34)$$

147 Here, $i = 0, 1, 2, 3, \dots, M$ and $j = 0, 1, 2, 3, \dots, N$



148
149 **Fig. 2. Specifying initial and boundary conditions**

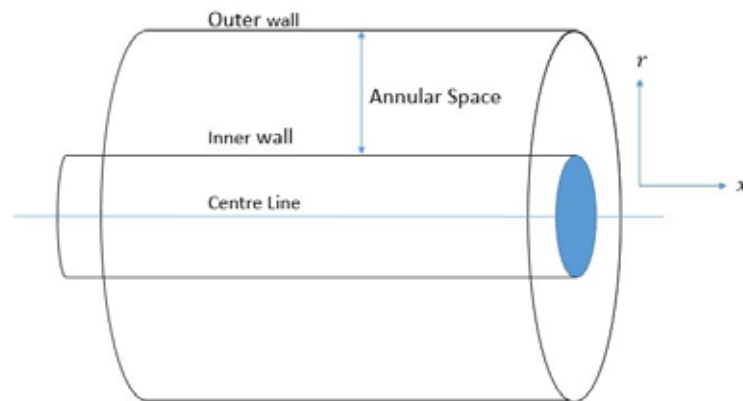
150 Figure (2) shows the discretization of the annular and the known initial boundary values of grid points.
151 Using boundary conditions values are obtained at the grids of the inner wall and outer wall and the
152 initial condition values are used for $t = 0$. Hence, subsequent values are approximated

153
154

155 3. RESULTS AND DISCUSSION

156
157
158
159

Finite difference method was programmed in MATLAB to visualize the suddenly stopped axial Couette flow for various cases between the inner pipe and outer pipe in the central symmetry plane (annular space).



160
161 **Fig. 3. Schematic description of annular space in axial direction.**

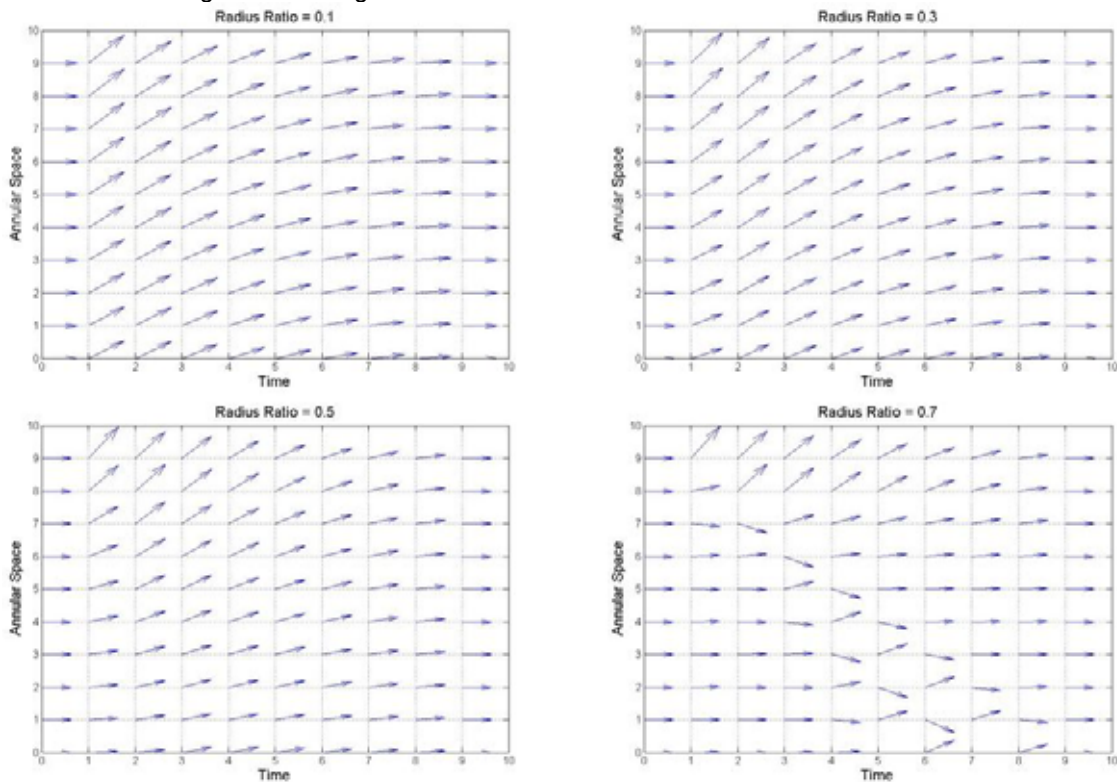
162

163 3.1 Case I

164
165
166

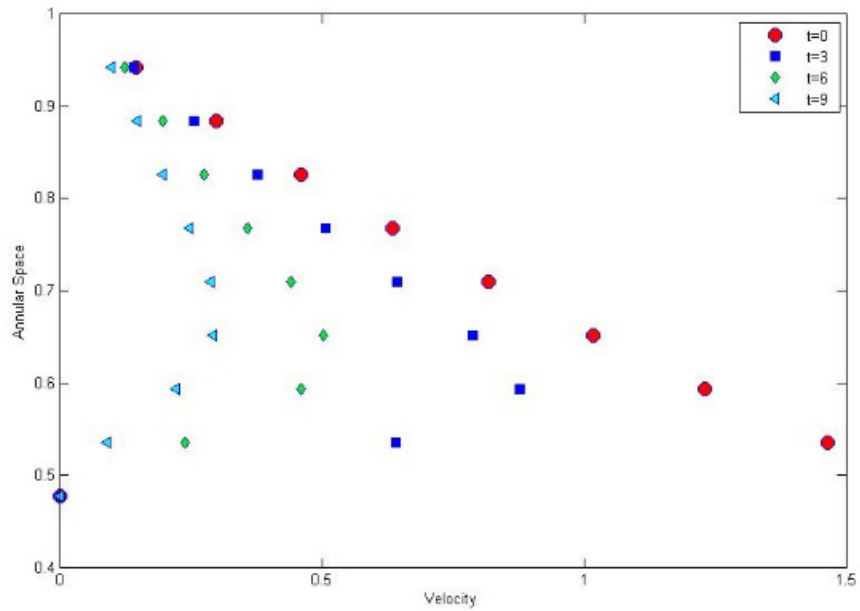
In this case the outer pipe was fixed and the inner pipe was moving at a constant velocity in axial direction and the inner pipe was suddenly stopped.

167 Figure (3) shows the streamlines at different radii ratios (η), 0.1, 0.3, 0.5 and 0.7 when initially the
 168 inner pipe was moving and suddenly the inner pipe was brought to rest. With respect to the radius
 169 ratios there is a significant change in streamlines of the flow field.



170
 171 **Fig. 4. Streamline for suddenly stopped axial Couette flow at different radius ratios for Case I**
 172 **when inner pipe moving at a constant velocity and outer pipe at rest (Time and annular space**
 173 **are non-dimensional)**

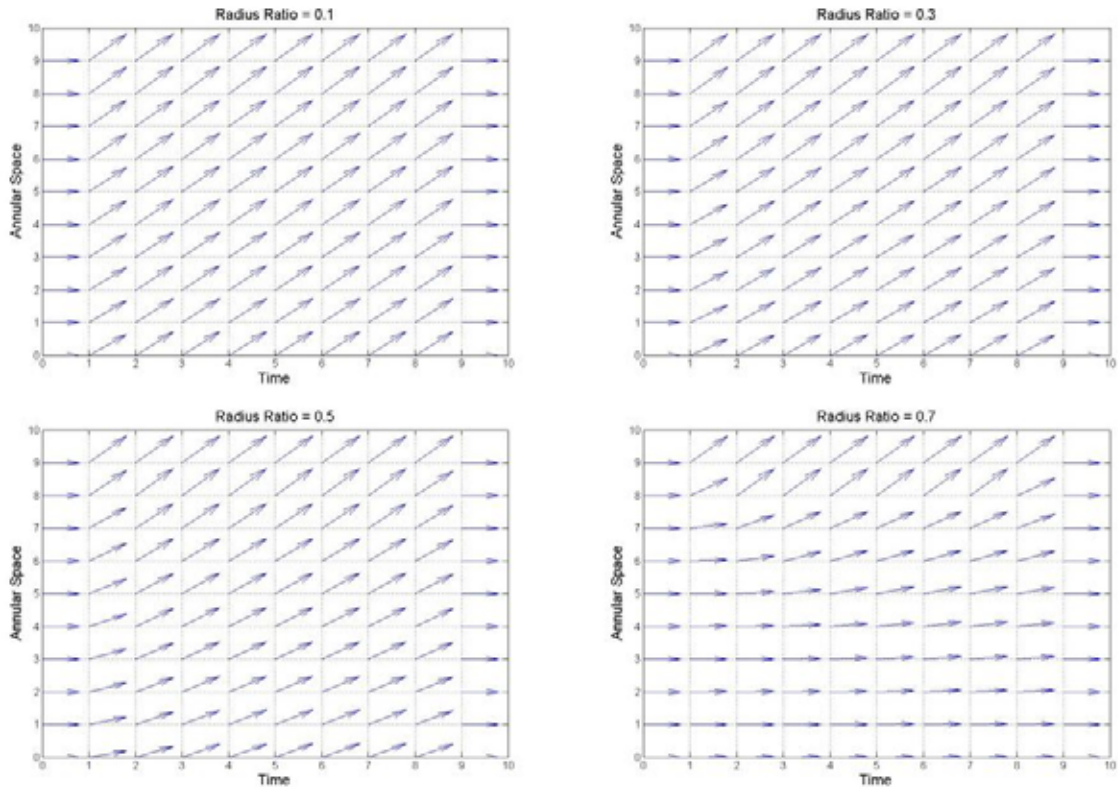
174 Figure (4) shows the points of discrete values of velocity profile at different time steps. Due to the
 175 viscosity of the fluid, near to inner boundary velocity was maximum and at the outer boundary the
 176 velocity was zero. Initially inner pipe was moving at a constant velocity and outer pipe was at rest.
 177 Then, the inner pipe was brought to rest suddenly. There was a decay in velocity profile was observed
 178 with respect to time.



179 Fig. 5. Velocity profiles at different times for Case I when initially inner pipe moving at a
 180 constant velocity and outer pipe at rest at $\eta = 0.477$ (Velocity and annular space are non-
 181 dimensional)
 182

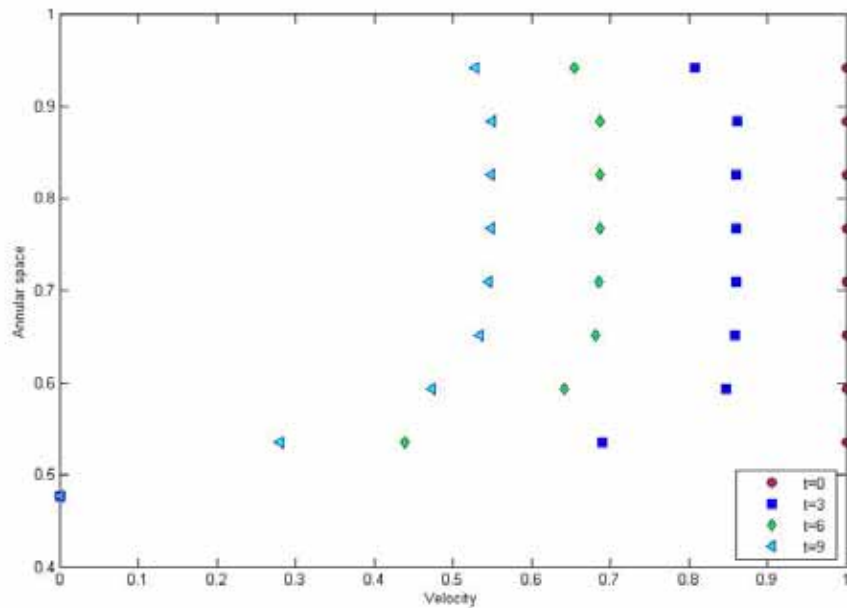
183 3.2 Case II

184
 185 When inner pipe and outer pipe were moving at a constant velocity and both pipes were suddenly
 186 stopped.
 187 For the different radius ratios (η), 0.1, 0.3, 0.5 and 0.7, streamlines of the suddenly stopped Couette
 188 flow is obtained when initially inner pipe and outer pipe is moving at a constant velocity. Figure (5)
 189 shows the flow field at different radius ratios. With respect to the radius ratios notable difference in the
 190 streamlines of the flow field is noticed.



191 **Fig. 6. Streamline for suddenly stopped axial Couette flow at different radius ratios for Case II**
 192 **when initially inner and outer pipes moving at same constant velocity (Time and annular space**
 193 **are non-dimensional)**
 194

195 Figure (6) represents the points of discrete values of velocity profile at different time steps. In this
 196 case inner and outer boundaries are moving at a constant velocity. Boundaries are moving with the
 197 same velocity and asymmetry in the velocity profiles are observed.

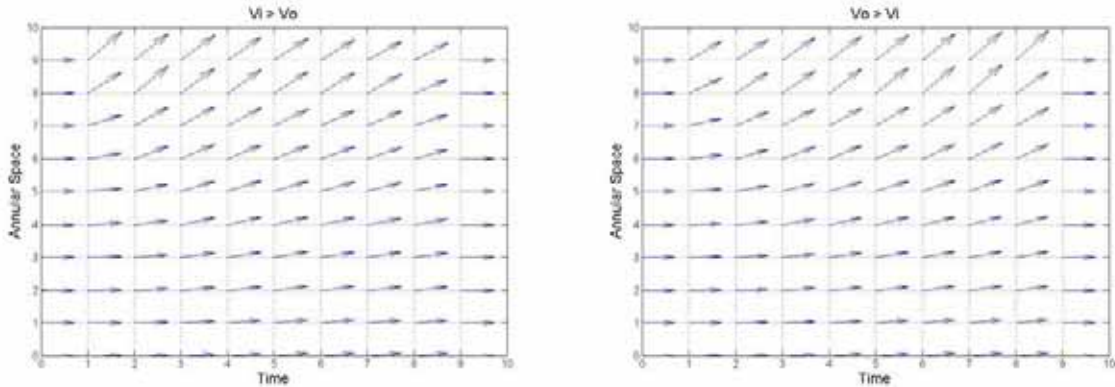


199 Fig. 7. Velocity profiles at different times for Case II when initially inner and outer pipes
 200 moving at same constant velocity at $\eta = 0.477$ (Velocity and annular space are non-
 201 dimensional)

202 **3.3 Case III**

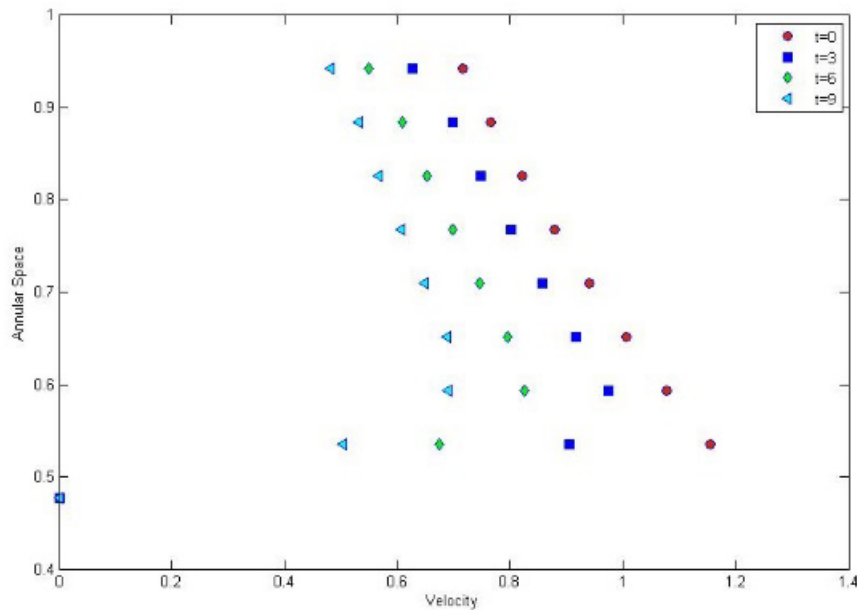
203 When inner pipe and outer pipe initially moving at different velocities (V_i and V_o) and both pipes are
 204 stopped suddenly.

205 Figure (7) denotes the streamlines of the abruptly stopped axial Couette flow when inner boundary
 206 and outer boundary have different constant velocities. In the flow field the change in streamlines are
 207 significant.



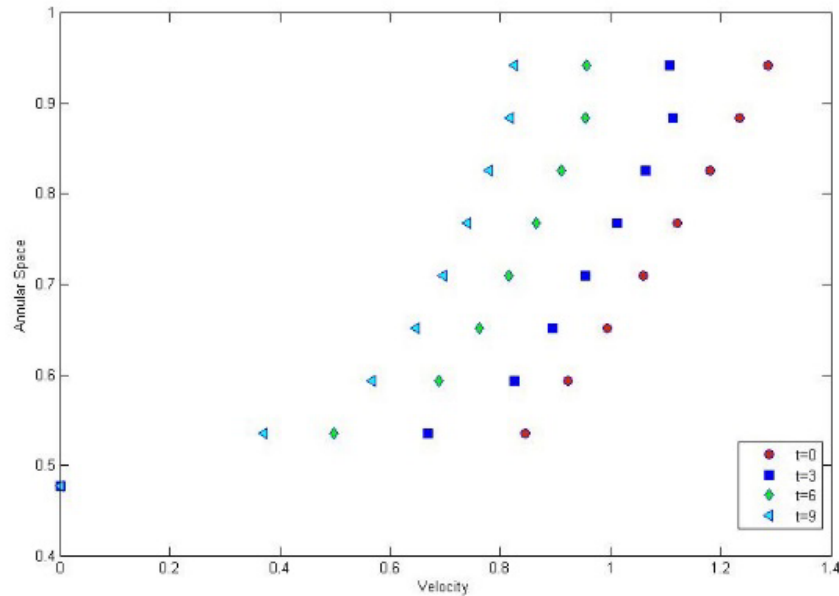
208
 209 Fig. 8. Streamline of suddenly stopped axial Couette flow for Case III when inner and outer
 210 pipes in different constant velocities (Time and annular space are non-dimensional)

211 Figure (8) shows the points of discrete values of velocity profile at different time steps when initially
 212 inner boundary moving faster than outer boundary and both are brought to rest suddenly.



213
 214 Fig. 9. Velocity profiles for abruptly stopped pipes at different times for Case III when $V_i > V_o$
 215 at $\eta = 0.477$ (Velocity and annular space are non-dimensional)

216 Figure (9) represents the points of discrete values of velocity profile at different time steps when
 217 initially outer boundary moving faster than inner boundary and both are suddenly stopped.



218
219 **Fig. 10. Velocity profiles for abruptly stopped pipes at different times for Case III when $V_o > V_i$**
220 **at $\eta = 0.477$ (Velocity and annular space are non-dimensional)**

221 4. CONCLUSION

222
223 In the work presented, the second order non-homogeneous partial differential equation was solved to
224 obtain the solution for Couette flow. The numerical approximation for the unsteady abruptly stopped
225 axial Couette flow was modelled using FDM. Three different cases were analysed in MATLAB
226 programming, to visualize the flow field and streamline and velocity profiles at different time steps
227 were obtained.

228 In case I, initially the inner boundary was moving at a constant velocity and it was suddenly stopped.
229 Streamlines for various radius ratios (η), 0.1, 0.3, 0.5 and 0.7 were obtained in Figure (3). In case II,
230 initially inner and outer boundaries were moving at same constant velocity and both boundaries were
231 suddenly stopped. Streamlines for various radius ratios (η), 0.1, 0.3, 0.5 and 0.7 were obtained in
232 figure (5). In both cases significant differences in streamlines of the flow field were visualized. In case
233 III, initially inner boundary and outer boundary had different velocities. Streamlines were visualized in
234 figure (7).

235 Different cases play different role in the flow characteristics of the annular flow. Flow characteristics
236 were changed due to the asymmetry of velocity profiles and unsteadiness of flow field. The
237 asymmetry of the velocity profile was affected by different radius ratios. Unsteadiness in the flow field
238 was happened due to sudden changes in flow parameters. So, these sudden changes in the flow
239 parameter and different radius ratios play important roles in the stability of the flow.

240 This work presents the analytical and numerical solution and the approach for the solution for abruptly
241 stopped axial Couette flow. The stability analysis can be carried out to analyse the stability of the flow
242 when a small disturbance is introduced to the flow. Which may help to understand and predict the
243 instability. The non-linear stability analysis could help in understanding the transition to turbulent
244 process which is not addressed in this work. We plan to use MATCONT continuation software to
245 perform a non-linear stability analysis [17]. Non-concentric annulus with bidirectional flow may give
246 the solution for the real world applications with minimizing assumptions.

247 REFERENCES

- 248
249
250 [1] R. W. Hanks and J. M. Peterson, "Complex transitional flows in concentric annuli," *AICHE J.*,
251 vol. 28, no. 5, pp. 800–806, Sep. 1982.
252 [2] Y. Wang and G. A. Chukwu, "Unsteady Axial Laminar Couette Flow of Power-Law Fluids in a
253 Concentric Annulus," *Ind. Eng. Chem. Res.*, vol. 35, no. 6, pp. 2039–2047, Jan. 1996.
254 [3] E. P. F. de Pina and M. S. Carvalho, "Three-Dimensional Flow of a Newtonian Liquid Through

- 255 an Annular Space with Axially Varying Eccentricity," *J. Fluids Eng.*, vol. 128, no. 2, p. 223,
256 2006.
- 257 [4] D. Das and J. H. Arakeri, "Transition of unsteady velocity profiles with reverse flow," *J. Fluid*
258 *Mech.*, vol. 374, pp. 251–283, 1998.
- 259 [5] D. DAS and J. H. Arakeri, "Unsteady Laminar Duct Flow With a Given Volume Flow Rate
260 Variation," *J. Appl. Mech.*, vol. 67, no. June 2000, pp. 274–281, 2000.
- 261 [6] M. E. Erdoğan, "On the flows produced by sudden application of a constant pressure gradient
262 or by impulsive motion of a boundary," *Int. J. Non. Linear. Mech.*, vol. 38, no. 5, pp. 781–797,
263 2003.
- 264 [7] A.-S. Yang and T.-C. Kuo, *Blowdown and fluid hammer studies for a satellite reaction control*
265 *subsystem*, vol. 215. 2001.
- 266 [8] T. Fukuchi, "Numerical calculation of fully-developed laminar flows in arbitrary cross-sections
267 using finite difference method," *AIP Adv.*, vol. 1, no. 4, p. 42109, Dec. 2011.
- 268 [9] P. Dutta and N. Nandi, "Study on pressure drop characteristics of single phase turbulent flow
269 in pipe bend for high reynolds number," *ARPJ J. Eng. Appl. Sci.*, vol. 10, no. 5, pp. 2221–
270 2226, 2015.
- 271 [10] A. Nayak, "On one dimensional unsteady flow through pipe and annular region between two
272 concentric pipes for a given volume flow rate variation: Exact solution and three dimensional
273 linear stability analysis," IIT, Kanpur, 2005.
- 274 [11] M. Dibakar, "Exact solution and linear stability analysis of unsteady sliding Couette-Poiseuille
275 flow," IIT, Kanpur, 2012.
- 276 [12] K. Ashok, "Instability of unsteady annular pipe flow: Theoretical and experimental
277 investigation," IIT, Kanpur, 2012.
- 278 [13] F. M. White, "Viscous Fluid Flow Viscous," *New York*, vol. Second, p. 413, 2000.
- 279 [14] J. Harrison, "Fast and Accurate Bessel Function Computation," in *2009 19th IEEE Symposium*
280 *on Computer Arithmetic*, 2009, pp. 104–113.
- 281 [15] W. G.A., *A treatise on the theory of Bessel functions.*, 2nd ed. Cambridge University Press,
282 1944.
- 283 [16] C. M. Bender and S. A. Orszag, *Advanced Mathematical Methods for Scientists and Engineers*
284 *I*. New York, NY: Springer New York, 1999.
- 285 [17] M. Spiegel, *Schaum's Outline of Laplace Transforms*. McGraw-Hill, 1965.
- 286 [18] J. A. Weliwita, "Spiral Defect Chaos and the Skew-Varicose Instability in Generalizations of the
287 Swift-Hohenberg Equation," University of Leeds, 2011.
- 288